Diagnostic Measurements on a Highly Ionized, SteadyState Plasma

Andrew L. Gardner, William L. Barr, Raymond L. Kelly, and Norman L. Oleson

Citation: Physics of Fluids (1958-1988) **5**, 794 (1962); doi: 10.1063/1.1724448
View online: http://dx.doi.org/10.1063/1.1724448
View Table of Contents: http://scitation.aip.org/content/aip/journal/pof1/5/7?ver=pdfcov
Published by the AIP Publishing

plicated equipment in running condition have been invaluable, and their suggested improvements have resulted in greatly increased reliability of operation.

The continued interest and encouragement given by Drs. C. M. Van Atta and R. F. Post are gratefully acknowledged.

This work was performed under the auspices of the U. S. Atomic Energy Commission.

THE PHYSICS OF FLUIDS VOLUME 5, NUMBER 7 JULY 1962

Diagnostic Measurements on a Highly Ionized, Steady-State Plasma

ANDREW L. GARDNER, WILLIAM L. BARR,
RAYMOND L. KELLY*, AND NORMAN L. OLESON*
Lawrence Radiation Laboratory, University of California, Livermore, California
(Received January 12, 1962)

Techniques and results are given for various measurements made on a highly ionized helium plasma in a steady-state plasma system (which employs a longitudinal magnetic field of approximately 1 kilogauss). Neutral-particle pressures ranged from about 3×10^{-4} mm Hg near the source to about 10^{-5} mm Hg in the downstream region. Spectroscopic measurements showed principal impurities were C, N, and O ions (up to C^{3+}, N^{4+}, and O^{4+} states). Doppler broadening measurements of He^{+} $\lambda 4686$ revealed ion temperatures up to 10 eV. Probe measurements indicated electron temperatures up to 20 eV and maximum ion densities of a little over 10^{13} cm^{-3}. Microwave transmission measurements (at $\lambda = 4$ mm and 8 mm) gave supporting evidence that the electron density exceeds 10^{13} cm.

I. INTRODUCTION

THIS paper recounts various measurements that have been made on a helium plasma produced in the system previously described in the companion paper.[1] A plan view of the system is shown at the top of Fig. 1 on which are indicated the positions where the measurements were made. An axial magnetic field of about 1 kilogauss extends throughout most of the region and no electric fields are deliberately impressed outside of the discharge chamber (shown at the left end of the sketch).

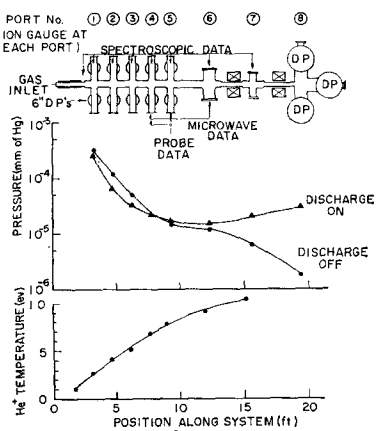

FIG. 1. Observation positions along the system and axial variation of neutral-helium pressure and helium-ion temperature.

The reported measurements do not represent a consistent set for a particular operating condition of the system, since they span a considerable period of time. Nevertheless, the general features of the plasma have proved to be notably reproducible and the data given are representative of typical operation.

II. NEUTRAL DENSITY ALONG THE SYSTEM

Eight ionization gauges (type VG-1A/2, made by Central Electronics Manufacturers, Inc.) were used to determine the neutral-particle distribution along the system. These were mounted vertically above the system axis at each port except 6 and 7 (Fig. 1), where they were mounted on the side flanges.

The gauges at ports 1 through 7 were magnetically shielded so that the presence of the magnetic field caused less than 3% change in the ion-current reading. The gauge at port 8 was unshielded, but its reading was affected less than 15% by the field.

In order to correct for individual variations in sensitivity, the ion gauges were compared against each other in a semistagnant helium atmosphere. This was done by closing off all pumps except that at one side of port 1 and adjusting the input helium flow to yield a pressure well above the base pressure.

A typical set of readings is shown in Table I.

* U.S. Naval Postgraduate School, Monterey, California
[1] L. S. Hall and A. L. Gardner, Phys. Fluids 5, 788 (1962).

TABLE I. Ion-gauge comparison and typical operating helium pressure (mm Hg).

Port	Comparison readings in semistagnant helium[a]	Factor to "correct" gauge to average reading	All pumps open (Readings have been multiplied by factor in column 3)		
			Base pressure (Impurity gases, no additional correction factor used)	Helium input of 280 micron liters/sec (Additional factor of 5 included to account for ion gauge efficiency in helium)	
				Discharge off	Discharge on
1	265×10^{-6}	1.12	0.85×10^{-6}	320×10^{-6}	260×10^{-6}
2	320	0.93	1.3	120	65
3	265	1.12	1.1	52	32
4	330	0.90	0.58	23	22
5	325	0.91	0.78	14	17
6	285	1.04	0.88	12	15
7	270	1.10	0.47	7.2	20
8	310	0.96	0.15	1.8	30

[a] Average reading 296, standard deviation 28, and expected deviation of mean 9.9.

Except for the column headed "base pressure," a factor of 5 has been applied to the ion-gauge readings to compensate for the low ionization efficiency in helium relative to air[2]; thus, the readings indicate real pressure. The values in the last two columns are plotted in Fig. 1. It should be noted that there are no pumps or restricting diaphragms in the region between ports 5 and 8. The effect of the discharge in transporting the gas, as ions, to the downstream portions of the system is readily seen. The rise in pressure at the downstream end indicates the burial system is not completely effective in pumping away the gas formed by the ions which recombine there, and a net backflow of neutral particles results. The reason for the rather high pressure (with the discharge on) in port 1 must be partly due to the recombination of ions which diffuse from the channel to the downstream side of the second cathode (1-in. aperture) or to the quartz diaphragm ($1\frac{1}{2}$-in. aperture) which precedes port 1. (The remaining quartz diaphragms have 2-in. or $2\frac{1}{2}$-in. apertures.) The fact that the lowest pressure occurs at port 6, where there are no diffusion pumps, is an indication that the plasma itself is serving as a pump for neutral particles.

III. SPECTROSCOPIC OBSERVATIONS

Spectra have been observed from the vacuum ultraviolet through the visible region for the purpose of studying the gross properties of the radiation. Spectrograms in the vacuum ultraviolet were made with a grazing incidence spectrograph[3] which operates at 82° angle of incidence, has a focal length of 1 m, and covers the range 50–2250 Å with a dispersion ranging from 3 Å per mm at 100 Å to 8 Å per mm at 2000 Å. A 3.4-m Ebert spectrograph with a dispersion of 5.2 Å per mm was used to identify the lines above 2000 Å.

A detailed analysis was made of the visible and near-ultraviolet spectrum observed through the quartz window in port 5. A total of 245 of the strongest spectral lines were measured in the range from 2000 to 5700 Å. Of these, 29 could not be identified, while another 29 had at least two possible identities. The remaining 187 lines were all due to one or another of the following: He, He^+, C^+, C^{2+}, C^{3+}, N^+, N^{2+}, N^{3+}, O, O^+, O^{2+}, or O^{3+}. Only He was deliberately admitted into the system. No metal which might have come from the discharge chamber was observed.

At port 3 (Fig. 1) the strongest lines of the following were observed with a 5-sec exposure on the vacuum spectrograph: He, He^+, C^{2+}, C^{3+}, N^{2+}, N^{3+}, N^{4+}, O^+, O^{2+}, O^{3+}, O^{4+}. With longer exposures, strong lines of C^+ appear along with weaker lines of the other ions listed above. Figure 2 shows a

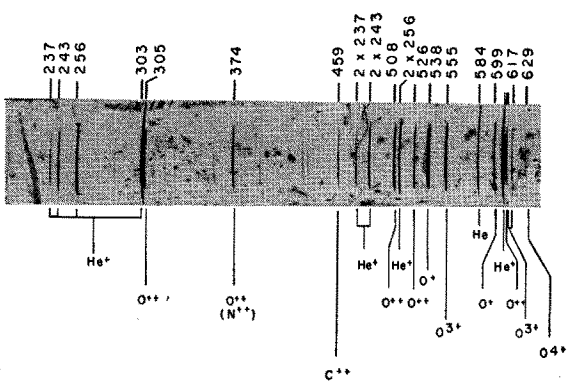

FIG. 2. Portion of vacuum ultraviolet spectrum at port 3.

[2] D. Alpert, in *Handbuch der Physik*, edited by S. Flügge (Springer-Verlag, Berlin, 1958), Vol. 12, p. 616.

[3] R. L. Kelly, "A Grazing Incidence Vacuum Spectrograph of Simple Design," UCRL-5924-T (1960, unpublished).

TABLE II. Spectra (underscored) observed in the radiation. (Ionization energy is given in eV.)

He	24.5	He^+	54.2							
C	11.2	C^+	24.3	C^{++}	47.7	C^{3+}	64.2	C^{4+}	392	
N	14.5	N^+	29.5	N^{++}	47.2	N^{3+}	77.1	N^{4+}	97.5	N^{5+} 552
O	13.6	O^+	35.0	O^{++}	54.7	O^{3+}	77.1	O^{4+}	113.4	O^{5+} 137.5

portion of the spectrum. The Lyman series in He^+ is much more intense, even in second order, than is the principal series in He. Quantitative estimates of the degree of ionization have not been made by this means, however.

The observation of O^{4+} shows that there are electrons present with energies of at least 77 V, while the absence of the spectrum of O^{5+} shows there cannot be many with energies as high as 114 V. The absence of the spectra of C^{4+} and N^{5+} does not indicate the absence of these ions because the high threshold for excitation prevents the production of their spectra, even though they are probably present. Table II displays those ions (underscored) whose spectra have been identified in radiation from the plasma.

For temperature measurement, the spectrum was photographed at port 6 using a Fabry-Perot interferometer crossed with a large prism spectrograph. Figure 3 shows one such interferogram taken with a 1.59-mm spacer (chosen to give a spectral range of 0.69 Å between fringes at 4686 Å). The Doppler width of this He^+ line is 0.53 Å, corresponding to an ion temperature of about 8 eV. There was no observable line shift or change in width when the direction of observation was changed from 90° to 45°, demonstrating that the ion velocities were oriented isotropically.

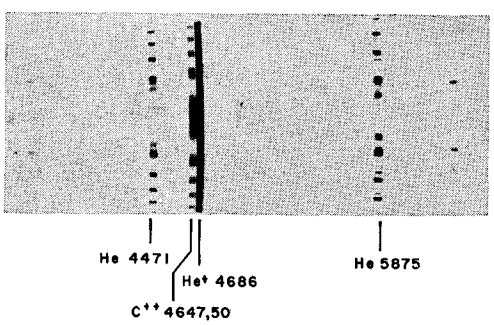

FIG. 3. Fabry-Perot interferogram at port 6 showing Doppler broadening of helium-ion line at 4686 Å (1.59-mm spacer).

Accurate measurements of the widths of the strongest spectral lines were made by directly scanning the interferometer patterns. For this a Fabry-Perot interferometer was crossed with a fast monochromator. The fringes were focused on a diaphragm which allowed the photomultiplier to view only a small area at the center of the fringe system. Scanning was accomplished by varying the gas pressure in the interferometer chamber. (This technique has been described by Biondi[4] and others.) Linewidths in excess of those due to fine structure and instrumental broadening were entirely due to Doppler broadening.

A study of the variation of the He^+ temperature along the axis of the system revealed a gradual increase in ion temperature with distance from the source. The lowest temperature observed was 1.1 eV at the position of the window in the discharge chamber. The highest was about 10 eV in port 7. The results are shown plotted in Fig. 1. This is consistent with the view that the ions are heated by collisions with the electrons along the entire length of the plasma, whereas the major loss of ions and ion energy is at the cathode of the discharge chamber.

An investigation of the ion lines in the spectrograms taken at port 5 with the Ebert spectrograph disclosed no indication of any gross rotation of the beam. Rotational velocities comparable with thermal velocities would have been detectable by the Doppler shifts produced. To gain higher resolution, interferograms were taken by collecting the light from horizontal strips about 0.7 mm thick at distances 1.0 to 1.4 cm above and below the beam axis at port 5, also 1.2 cm above and below the axis at port 6. Again, no Doppler shifts were detected, although shifts equal to one-tenth of the linewidths would have been seen. Thus, gross rotational velocities, in those parts of the beam which were studied optically, are less than 5×10^5 cm/sec.

The visible spectrum was scanned at ports 1, 2, 4, and 5 using a fast monochromator with a photomultiplier detector (under uniform conditions) to ascertain the relative intensities of any particular line at the various positions. The intensities of the neutral helium lines were proportional (within roughly 30%) to the ion-gauge readings at the various locations, thus indicating no appreciable falloff in the density of the exciting electrons. The He^+ λ4686 line intensity, however, was more nearly constant, diminishing by only about a factor of $\frac{1}{2}$ from port 1 to port 5. The latter decrease may be

[4] M. A. Biondi, Rev. Sci. Instr. **27**, 36 (1956).

attributed to two causes: a reduction in the density of exciting electrons (energy more than 50 eV), and/or a reduction of He^+ due to diffusion or to second ionization.

Radial distributions of excited ions and neutrals in the beam have been deduced from beam profile measurements of He^+ λ4686 and He λ5875. The profiles were determined by scanning vertically across the beam using a monochromator equipped with an image rotator to make the beam image parallel to the entrance slit. The radial distributions obtained at port 4 are shown in Fig. 4, where $f(r)$ is the density of emitters (normalized to unity at $r = 0$) which is proportional to the product of the ion (or neutral) density and the effective density of electrons of sufficient energy to cause the excitation.

An interesting profile is observed in the neutral

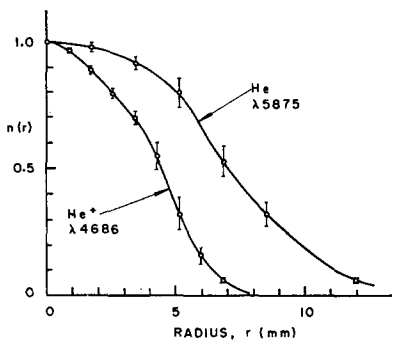

FIG. 4. Radial intensity distributions from beam-profile measurements at port 4.

He spectral line λ5015 ($2^1S - 3^1P$) in those regions where the gas pressure is high enough, such as at port 1. There the beam profile in this line shows a pronounced wing which is visible as a "green glow" throughout the surrounding region. Because of the long lifetime of the 2^1S metastable state (the lifetime is determined primarily by the frequency of collisions with the walls), the resonance fluorescence of λ5015 is probably strong. The population of the metastable state is maintained by the photoexcitation of the n^1P states followed by the decay from the ^1P to the metastable 2^1S state with some λ5015 produced in the process. The phenomenon of the green glow in certain discharges in He was thoroughly investigated by Lees and Skinner in 1932.[5]

IV. PROBE MEASUREMENTS

Cylindrical electrostatic probes have been used in the plasma to obtain information on electron temperature, ion density, and plasma potentials. One type of probe used with success in the outer

[5] J. H. Lees and H. W. B. Skinner, Proc. Roy. Soc. (London) **A137**, 186 (1932).

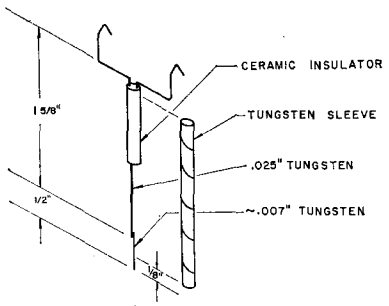

FIG. 5. The "stationary" Langmuir-probe design.

regions is shown in Fig. 5. The active portion is tungsten wire $\frac{1}{8}$ in. long and a few mils in diameter. The stem is shielded by an electrically floating tungsten tube or, in some cases, by a ceramic insulator. A two-fingered hook, operated through a Wilson seal, is used to pick up any one of several probes from a storage shelf within the vacuum system and move it to the desired position within the plasma where it hangs vertically. Such probes can thus be interchanged quickly without the necessity of shutdown of the system.

The heat input to the probe, and hence its equilibrium operating temperature, is lowest when the net collection current is small, i.e., when the probe is near floating potential. Use of a stationary probe is limited to the outskirts of the plasma column since even an electrically floating probe is melted in the plasma interior. At all radial positions, however, precautions must be taken to avoid melting the probe when the current–voltage characteristic is being explored. A practical solution is to focus the image of the probe upon a light-sensitive detector which in turn operates a relay that disconnects the power supply from the probe when the danger point is reached. In the meantime the current–voltage characteristic is displayed on an oscilloscope and photographed. It is obvious that a faster voltage sweep allows a larger portion of the curve to be covered before the probe temperature becomes excessive.

Figure 6 shows typical probe-characteristic curves taken by first sweeping the voltage from the floating potential downward until the safety relay operated, then resetting it and sweeping from floating potential upward until the safety relay again opened the circuit. (For simplicity in establishing the current zero, the supply voltage is continuously applied to the oscilloscope even after the probe has been disconnected.) In the "ion current" region shown at the left, the useful portion of the curve is ultimately limited by excessive electron emission (which has the appearance of increased ion collection) well

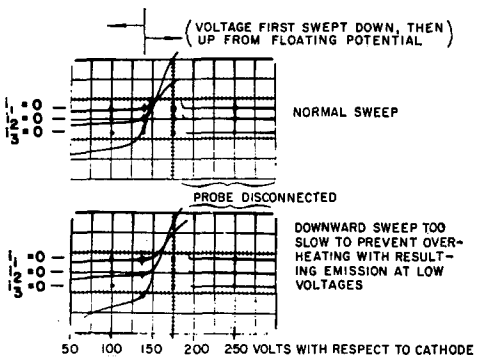

FIG. 6. Probe current-voltage characteristic curves showing three simultaneous traces of the same current ($i = i_1 = i_2 = i_3$) with vertical sensitivities: i_1 = 250 mA/division; i_2 = 100 mA/division; i_3 = 25 mA/division.

before the probe is in danger of melting. The drooping of the curves near the left side in the lower diagram of Fig. 6 is the result of this thermionic emission of electrons by the probe. The flat portions of the traces on the right in Fig. 6 occur after the safety relay operated and no current was being collected by the probe.

Since the probe measurements are made in the presence of a strong magnetic field, the small gyroradius of the electron invalidates the use of conventional Langmuir theory[6] for the analysis of saturation electron current to the probe. Although this objection does not apply to the ions in this system because of their much larger gyroradius, Wenzl,[7] and also Bohm, Burhop, and Massey,[8] have found that, in the application of Langmuir's theory to the collection of ions, one should use for the ion temperature an effective value which may be quite different from the actual ion temperature. However, if one is interested only in ion density, a knowledge of the actual or effective ion temperatures is not required.

For cylindrical probes drawing orbital-motion-limited currents, the theory developed by Langmuir and Mott-Smith,[9] indicates that the ion density n_i is proportional to the square root of the slope of the plot of I^2 vs V for sufficiently negative voltages (with respect to plasma potential) and sufficiently large ratios of sheath radius to probe radius, i.e.,

$$dJ_i^2/dV = -(2e^3/\pi^2 m_i)n_i^2, \qquad (1)$$

where J_i is the ion current density to the probe and m_i is the mass of the ion.

The conditions in the present experiment do not satisfy the Langmuir–Mott-Smith criteria for current limitation to the probe by orbital motion, i.e., that the ratio of the sheath radius to the probe radius should be much greater than unity. However, Hall of LRL has pointed out the possibility of orbital-motion limiting taking place in the region of small potential variation outside the sheath in such a way as to preserve the analytic form of the probe voltage–current characteristic of the original theory, provided the mean free path is large compared to probe and sheath dimensions. (This would be consistent with the experimental data since the probe plots do show this analytic *form* rather well.) In such a case a correction factor would be needed in order to properly apply the original cylindrical probe relationship given by Langmuir and Mott-Smith for the measurement of ion density. The correction factor may be expected to be of the order of T_i/T_e which, for the case of the present measurements, is of the order of unity.

Experimentally, the plot of I^2 vs V does approach a constant-slope asymptote at large negative values of voltage as can be seen in the three typical plots in Fig. 7. However, the magnitude of the slope is influenced by the presence of the shield, one reason being that the shield intercepts some ions which would otherwise be collected by the probe. The effect of an additional (dummy) shield is shown in Fig. 8 for one position in the outskirts of the plasma. In this case the added perturbation decreased the indicated value of ion density about 20%. This experiment has not been repeated for the interior of the plasma where recent techniques have employed an insulating shield of boron nitride (BN) that tapers to a diameter of about 40 mils near the active region of the probe.

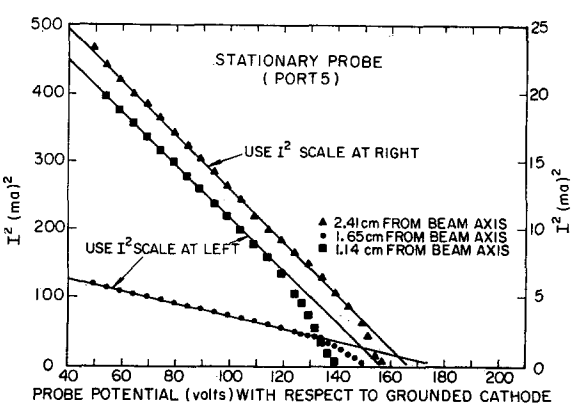

FIG. 7. I^2 vs V (for V less than floating potential).

[6] I. Langmuir and H. Mott-Smith, Jr., Gen. Elec. Rev. **27**, 449, 538, 616, 762, 810 (1924).
[7] F. Wenzl, Z. angew. Physik **2**, 59 (1950).
[8] D. Bohm, E. H. S. Burhop, and H. S. W. Massey in *Characteristics of Electrical Discharges in Magnetic Fields*, edited by A. Guthrie and R. K. Wakerling (McGraw-Hill Book Company, Inc., New York, 1949), Chaps. 2 and 3.
[9] Reference 6, p. 455.

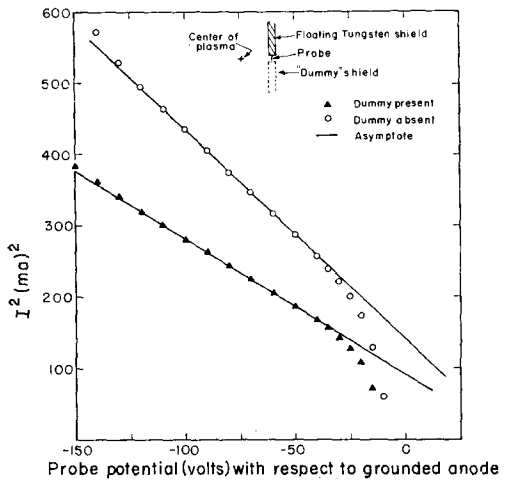

FIG. 8. I^2 vs V, effect of added perturbation.

The asymptote of the I^2 vs V plot is used to extrapolate in order to obtain the ion current in regions where ion and electron currents are comparable. This value is algebraically subtracted from the total current, at a particular probe voltage, to derive the collected electron current.

Electron temperatures are determined by the retarding-field method, a procedure generally believed to give valid results even in the presence of the magnetic field. Figure 9 shows that in the outskirts of the plasma the presence of an additional "shield" has little effect on the indicated electron temperature. From this, one infers that the original shield likewise has little effect on the measured value of the electron temperature.

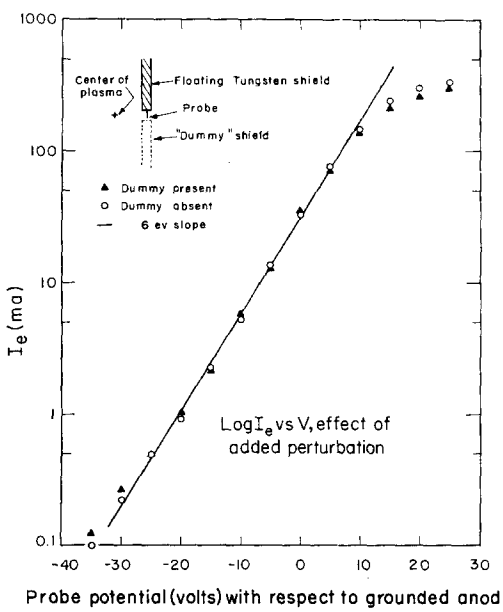

FIG. 9. Log I_e vs V, effect of added perturbation.

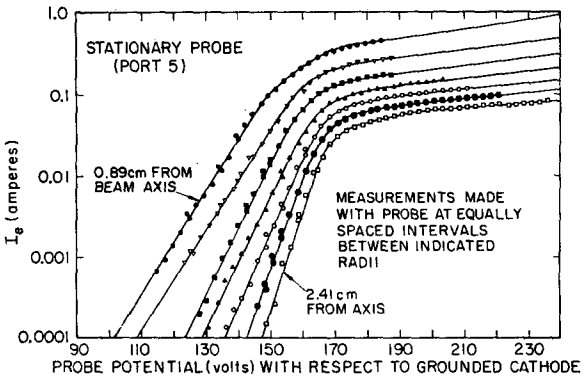

FIG. 10. Log I_e vs V for various radial distances from the axis.

Figure 10 shows several semilog plots of electron current to the probe at various distances from the axis of the plasma column. As previously noted, the inner portions of the plasma are inaccessible to the stationary probe.

Figure 11 shows the rudiments of an assembly in which one or more probes are mounted in spoke fashion on a rotating axle in order to lower their duty ratio in the plasma. This permits the plasma to be explored all the way to the axis without undue heating. Actually, the hub on which the probes are mounted consists of two insulated halves, and an electrical connection is made at each end of the short rotating shaft. This permits the use of single or double probes, although only single probes have been used with the rotator to date. One or more timing pulses per revolution are generated by light reflected from mirrors mounted on the shaft of the driving motor, which runs at about 900 rpm. The bearings and parts near the plasma are shielded to an extent by stainless-steel sheets which are electrically floating.

A photograph of the head of the rotator assembly is shown in Fig. 12. In this instance, the stem of the top probe is shielded with a BN tube which is held in place with a small chuck that floats

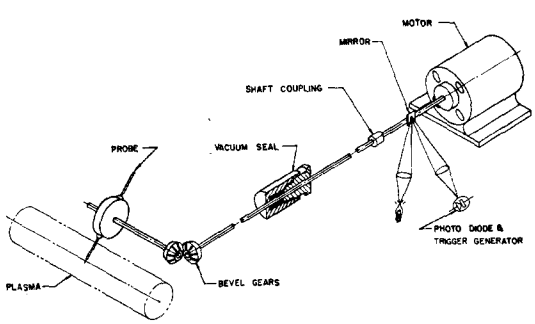

FIG. 11. Elements of the rotating probe assembly.

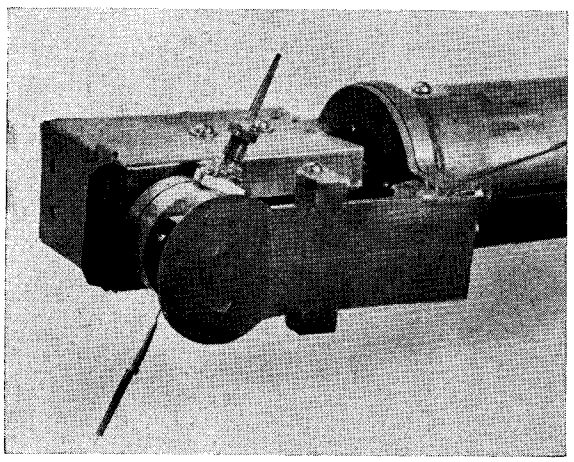

FIG. 12. Photograph of the head of the probe rotator.

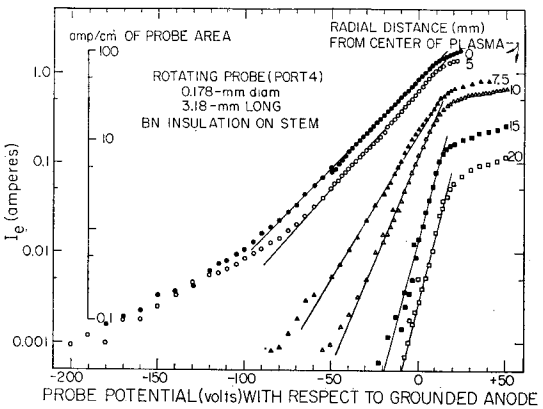

FIG. 14. Log I_e vs V for various radial distances from the axis.

electrically. Other methods are also used to support the BN sleeve.

In order to obtain greater voltage excursion without melting the probe, it is desirable to allow the probe to cool (at floating potential) for one or two revolutions after each pass when current has been collected. A circuit for accomplishing this is shown schematically in Fig. 13. This arrangement illuminates one spot on the characteristic curve on each active pass of the probe through the selected position (determined by the time delay) in the plasma, and in a matter of a few minutes an entire curve is "painted" on a time-exposure photograph of the scope. With this method the electron saturation region may be reached even at the axis of the plasma with probes of only a few mils diameter.

Semilog plots of the electron current to the probe as a function of the probe potential are shown in Fig. 14 for various radial distances from the axis of the plasma column at port 4. The knee in the upper part of each curve occurs in the vicinity of the space potential. The flattening of the left portion of the two upper curves is one indication of the presence of some higher-energy electrons in the central core of the plasma (which magnetically maps into the region inside the discharge chamber).[1] During these measurements the operating potential of the cathode (that feeds primary electrons into the discharge) was −165 V with respect to the grounded anode.

The radial variation of T_e, n_i, and the floating potential is indicated in Fig. 15, which shows the results of various measurements at ports 4 and 5 (cf. Fig. 1) for plasma conditions that were not identical. For the calculation of ion density it was assumed that only singly charged helium ions were present, and Eq. (1) was used despite the previously noted question of its applicability to this case.

A few on-axis measurements were made with the rotating probe at ports 1 and 2. The data showed no pronounced differences from the probe measurements made at ports 4 and 5.

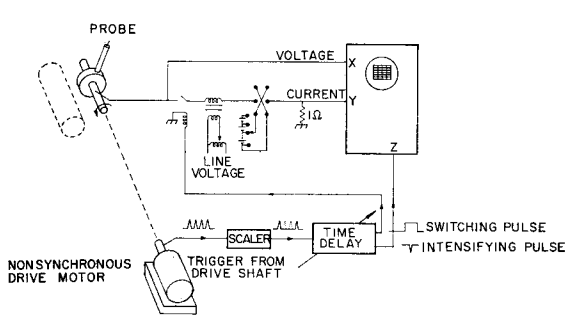

FIG. 13. A voltage-sweep circuit for the rotating probe.

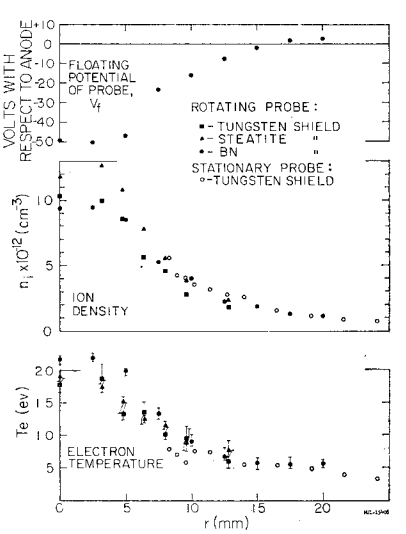

FIG. 15. Radial variation of V_f, n_i, and T_e. Rotating probe (port 4): Tungsten and steatite shields—earlier data using a series of fixed voltages; BN shield—"continuous" voltage scan. Stationary probe (port 5): still earlier data.

V. MICROWAVE MEASUREMENTS OF ELECTRON DENSITY

Microwave methods have been employed in the magnetic-channel region to measure the approximate electron density, and to serve as a monitor of performance during operation of the system. Transmitter and receiver horns pass a microwave beam transversely through the plasma column with the E field of the wave parallel to the magnetic field of the system. The presence of plasma causes both a phase change and an attenuation of the microwave beam. Measurements of these quantities at appropriate frequencies yield information on the electron density in the plasma,[10] although in no case can the spatial resolution be better than the order of a free-space wavelength.

Originally, 25-kMc (λ = 12 mm) beams from a common source were used simultaneously at ports 1, 2, 4, and 5 (Fig. 1). With such an arrangement, before the highly ionized plasma was achieved, the electron density was observed to decrease monotonically with distance from the discharge chamber, falling about an order of magnitude from port 1 to port 5. In present operation, however, measurements indicate the plasma density is more nearly uniform. No 25-kMc measurements have been made during recent operation, since the electron density is now well above the cutoff value for this frequency.

The significance microwave data on the present system have been taken at port 6 and more recently at port 4 as follows:

Port 6

Two microwave beams (λ = 4 and 8 mm) were transmitted through the same portion of the plasma on different diameters (separated azimuthally about 16°). All four horns were cantilevered from a common adjustable support, as shown in Fig. 16, which allowed them to be appropriately centered on the plasma.

8-mm Beam

The two horns of 1.25-in. (transverse) × 1-in. (axial) aperture have a separation of 8 in. At 35 kMc the presence of the plasma introduces an attenuation of 12 to 30 dB. Maximum attenuation occurs when the horns are somewhat misaligned with the plasma (presumably a result of diffraction effects). The phase shift varies and is difficult to measure because of the severe attenuation.

[10] S. Glasstone and R. H. Lovberg, *Controlled Thermonuclear Reactions* (D. Van Nostrand Company, Inc., New Jersey, 1960), p. 170 ff.

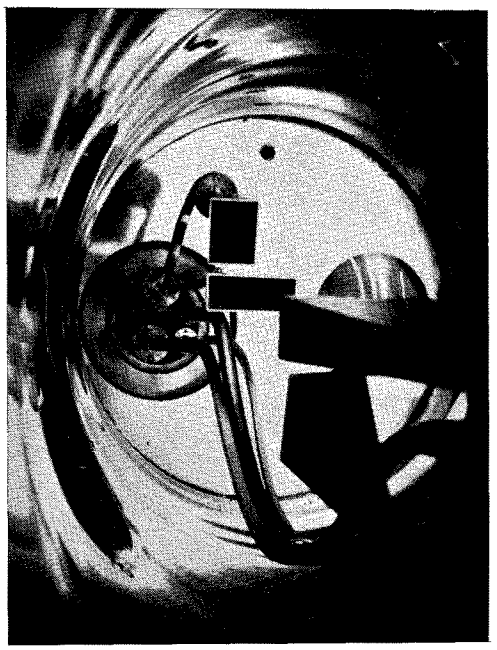

FIG. 16. Horns for 8- and 4-mm waves, cantilevered from an adjustable support.

4-mm Beam

The two horns of 0.75-in. (transverse) × 2-in. (axial) aperture are separated a distance of 8 in. At 70 kMc the presence of the plasma introduces a phase shift of approximately 180° with less than 1-dB attenuation.

Port 4

Spherical Lucite lenses were used to bring a transmitted 4.65-mm beam to an approximate focus at the axis of the plasma column (as sketched in Fig. 17). A phase shift of 175° was measured.

Since the low-frequency beam is approximately cut off, whereas the high-frequency beam is not, it is likely that the plasma frequency of the core lies between 35 and 70 kMc. This brackets the electron density between 1.5×10^{13} and 6×10^{13} electrons/cm^3. The value of 1.5×10^{13} electrons/cm^3 and the observed pressure of 1.5×10^{-5} mm of Hg at port 6 (cf. Table I) would correspond to about 97% ionization of helium if only singly charged ions were formed.

The lack of good spatial resolution in the microwave measurements requires an assumption regarding the radial distribution of electron density. However, the high-density region near the axis makes the dominant contribution to the phase shift, and since this region is at most only a few wavelengths thick it is reasonable to represent the plasma

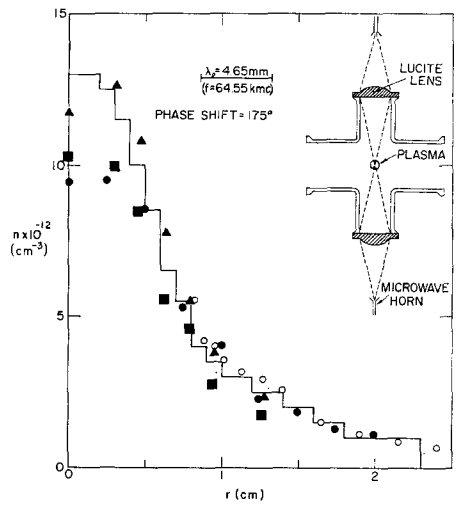

FIG. 17. A stepped distribution of electrons which would produce 175° phase shift of a perfectly focused 4.65-mm beam. (Probe measurements of approximate ion density are shown for comparison.)

by a homogeneous slab of given thickness. In such a case the phase shift ϕ is given by

$$\phi = \frac{\text{thickness}\,[1-(1-\omega_p^2/\omega^2)^{\frac{1}{2}}]}{\text{free-space wavelength}} \times 360°, \qquad (2)$$

where ω_p is the angular plasma frequency, and ω is the angular frequency of the microwave beam.

If the plasma at port 6 is assumed to be equivalent to a uniform slab 1 cm thick, the observed phase shift of 180° corresponds to an electron density of 2.3×10^{13} electrons/cm^3.

A more refined evaluation of the electron density may be made with the measurement of 175° phase shift at port 4, where probe measurements have given an indication of the radial distribution of ions. If one neglects the effects of poor focusing (and the use of spherical instead of cylindrical focusing) the resulting phase shift may be used to give an absolute value to any assumed relative radial electron distribution. By using the probe measurements of ion density at port 4 as an indication of the radial distribution of electrons, a stepped distribution of electron density has been synthesized which would yield the observed phase shift. This is shown in Fig. 17, which also reproduces the probe data from the center graph of Fig. 15.

The remarkably close agreement with the probe measurements is no doubt partly fortuitous. Aside from questions of validity of the probe analysis methods, the perturbing effect of the probe shield has been shown to decrease the indicated ion density (cf. Fig. 8). On the other hand, one might expect that imperfect focusing of the microwaves would decrease the observed phase shift.

ACKNOWLEDGMENTS

The authors wish to acknowledge the contribution of those whose assistance has been most appreciated. In particular, Laurence S. Hall participated in preliminary phases of most of the measurements and rendered valuable assistance in the interpretation of the probe measurements. Lt. Daune M. Gall (USN) performed much of the analysis for the early probe measurements, and William J. Stroh maintained and operated the complicated system throughout the course of the measurements.

Special thanks are also accorded to Dr. R. F. Post and Dr. C. M. Van Atta for their encouragement throughout the work.

This work was performed under the auspices of the U. S. Atomic Energy Commission.